Generic stacks and application of composite rules for the detailed sizing of laminated structures

G. Ntourmas[a,b,*], F. Glock[b], F. Daoud[b], G. Schuhmacher[b], D. Chronopoulos[a], E. Özcan[c]

[a]*Institute for Aerospace Technology & The Composites Research Group, The University of Nottingham, NG7 2RD, UK*
[b]*Stress Methods and Optimisation, Airbus Defence and Space GmbH, 85077 Manching, Germany*
[c]*Computational Optimisation and Learning Lab, The University of Nottingham, NG7 2RD, UK*

Abstract

Two-stage approaches are commonly applied to optimise the stacking sequence of large-scale composite structures. The two stages consist of a gradient and non-gradient based optimisation addressing the mixed nature of continuous and discrete constraints and design variables of the detailed sizing of laminated structures. For the two-stage process to be successful, all constraints from both stages should be fulfilled eventually. This study employs generic stacks to model the thickness and stiffness distribution of the structure. A generic stack is comprised of a collection of layers whose orientations are fixed *a priori*, but thicknesses can vary independently enabling exploration of the design space. To achieve a 'right first time' implementation and avoid burdensome iterations over both stages, a maximum amount of discrete design and manufacturing constraints should be considered in the

---

[*]Corresponding author
  Email address: `georgios.ntourmas@nottingham.ac.uk` (G. Ntourmas)

gradient-based optimisation stage. A special attention is paid to the continuity or blending constraint which can be formulated precisely using generic stacks. The results for a benchmark case show that the introduced two-stage approach can, not only satisfy all imposed constraints in a single iteration of the overall two-stage process but also yield a lower structural mass when compared to equivalent previously proposed approaches.

1. Introduction

Modern aeronautical structures are increasingly made out of fibre reinforced plastics, because these offer reduced weight and enhanced mechanical characteristics. However, designing large-scale composite structures poses two key challenges. The first one is linked to the fact that high computational resources are required to optimise real-world structures and the second to the nature of the detailed sizing of composite structures which involves both discrete and continuous design variables and constraints.

Many different approaches have been proposed over the past years [1, 2] concerning stacking sequence optimisation. Genetic algorithms [3, 4, 5, 6, 7] and other metaheuristics [8, 9, 10, 11] have been successfully applied as they can deal with both the continuous and discrete nature of the stacking sequence optimisation. The difficulty with such single-stage approaches lies with the limitations of applying them to real-world optimisation problems due to their required computational cost. Aircraft structures are sized by hundreds or thousands of load cases and that, in combination with a very

2

large number of design variables required to model the properties of the structure, leads to the need for many thousands optimisation iterations which come along with the costly computation of the structure's Finite Element model solution [12].

Gradient-based optimisation approaches can deal with the computational expense of large-scale problems but are better suited for continuous design spaces. For that reason, a non gradient-based optimisation algorithm can be employed in a following stage, to enable a discrete stacking sequence adhering to all composite design and manufacturing rules [13, 14]. Usually, lamination parameters [15] are employed to model the stiffness properties of the laminate. Many researchers [16, 17, 18] have used a gradient-based optimisation exploiting lamination parameters and a lot of work has been conducted to determine their feasible design space [19], enforce composite design guidelines [20, 21] and strength requirements [22, 23]. The reason for their wide acceptance is that they provide a compact formulation for the properties of a structural zone with a maximum of 12 design variables, in the most general case, plus an additional design variable for the thickness of the zone. The lamination parameter design space is convex [24] and buckling is a concave function [25]. However, when using lamination parameters one has no clear indication of the actual stacking sequence which leads to two major disadvantages. First of all, composite design guidelines whose formulation applies on a discrete ply level are hard to formulate or cannot be formulated accurately. Secondly, the formulation of first ply failure methods leads to more conservative failure envelopes, while progressive ply failure methods cannot be used to evaluate the strength of the laminate because the stacking

sequence is not yet known.

Polar parameters have also been used as an alternative to lamination parameters to describe the stiffness of the structure in a gradient-based optimisation [26, 27]. Polar parameters share the drawbacks mentioned for lamination parameters although work to address them has been conducted [28, 29].

Instead of using polar or lamination parameters a more direct approach is to model the laminate using design variables related to the actual ply properties e.g. thickness, fibre orientation or material. Even though recent work has proven that, against common belief, the feasible domain of lamination and polar parameters is not convex [30] when the thicknesses of the plies are restricted to manufacturable values, a parametrisation employing thicknesses or layer orientations presents a stronger non-convexity and introduces a design space with more local minima. Nonetheless, such parametrisations were amongst the first to be used and are still employed. Mateus et al. [31] used both layer thickness and orientation to optimise the buckling strength of a composite laminate. An optimisation with a fixed stacking sequence and only the thicknesses of the individual layers used as design variables was performed by Schmit Jnr. and Farshi [32] and two manufacturing constraints were included in the optimisation by Costin and Wang [33]. Most recently, such approaches have been mainly applied to the design of wind turbine blades [34]. Discrete Material Optimisation [35, 36] and Discrete Material and Thickness Optimisation [37, 38] employ design variables related to the thickness or material of a laminate. Their application has been limited to a small number of design variables per structural zone to keep the complexity

of the optimisation to a minimum.

The main novelty of the work lies in the usage of 'physical layers' to model not only the the thickness but also the stiffness distribution of the structure. Moreover, as many discrete composite rules as possible are implemented within this gradient-based optimisation framework. This modelling of the property will be referred to as a generic stack which is comprised of multiple layers of fixed orientation whose thickness can vary continuously. The motivation for using generic stacks is provided by the need to employ ply-based failure criteria and precisely accommodate discrete composite guidelines in the gradient based optimisation, the importance of which has been identified in the literature [39]. Combined with the developed second stage optimisation strategy [40], the presented two-stage process can consistently lead to stacking sequences which satisfy all required constraints in only one pass of the two-stage process. Besides that, application to a benchmark problem shows that the current methodology is able to achieve a lower structural mass compared to previous studies which share equivalent design criteria.

The rest of this paper is structured as follows: In Section 2 the two stages of the optimisation process are discussed with an emphasis on the modelling of the structural properties using generic stacks and the formulation of composite rules such as blending in the design space of generic stacks. Results from the application of the composite constraints and a comparison against literature results for an academic benchmark are demonstrated in Section 3. The findings of this work are summarised in Section 4.

2. Two-stage optimisation process

The developed two-stage optimisation process is discussed in this section. Particular emphasis is given on the first, gradient-based (continuous) stage and the incorporation of the composite design guidelines. Only a brief summary of the second, discrete optimisation stage is provided and the reader is invited to further reading for the complete formulation [40].

2.1. First stage: Continuous optimisation

In the first stage of the optimisation process, a gradient-based algorithm is employed to retrieve the optimal thickness and stiffness distribution of the structure. Generic stacks are used to parametrise the properties of each laminate. Physical constraints related to strength and buckling and composite constraints associated with the stacking sequence characteristics of the laminate are formulated for the design space of generic stacks.

2.1.1. Generic stacks parametrisation

A generic stack is comprised of multiple generic layers. The exact orientation and stacking sequence of these plies is fixed during the optimisation whereas the individual thickness of each generic ply corresponds to a design variable which can take any real positive value. Several generic plies are used to form a generic stack as shown in Fig. 1. The number and stacking sequence of the generic stack needs to be chosen so that the resulting thickness and stiffness does not depend on the modelling decisions. Knowing the stacking sequence and thickness of each generic ply, the extensional stiffness matrix A, the coupling stiffness matrix B and the bending stiffness matrix D can be calculated as:

$$A_{ij} = \sum_{k=1}^{n} \left(\bar{Q}_{ij}\right)_k (z_k - z_{k-1}) \tag{1}$$

$$B_{ij} = \frac{1}{2} \sum_{k=1}^{n} \left(\bar{Q}_{ij}\right)_k \left(z_k^2 - z_{k-1}^2\right) \tag{2}$$

$$D_{ij} = \frac{1}{3} \sum_{k=1}^{n} \left(\bar{Q}_{ij}\right)_k \left(z_k^3 - z_{k-1}^3\right). \tag{3}$$

In equations 1-3, z_k is the distance between and the midplane of the laminate and the side of the kth layer which is further away from the midplane. The elements of the transformed reduced stiffness matrix $\bar{Q}$ are calculated as:

$$
\begin{aligned}
\bar{Q}_{11} &= Q_{11} \cos^4 \theta + 2\left(Q_{12} + 2Q_{66}\right) \cos^2 \theta \sin^2 \theta + Q_{22} \sin^4 \theta \\
\bar{Q}_{12} &= Q_{12} \left(\cos^4 \theta + \sin^4 \theta\right) + \left(Q_{11} + Q_{22} - 4Q_{66}\right) \cos^2 \theta \sin^2 \theta \\
\bar{Q}_{16} &= \left(Q_{11} - Q_{12} - 2Q_{66}\right) \cos^3 \theta \sin \theta - \left(Q_{22} - Q_{12} - 2Q_{66}\right) \cos \theta \sin^3 \theta \\
\bar{Q}_{22} &= Q_{11} \sin^4 \theta + 2\left(Q_{12} + 2Q_{66}\right) \cos^2 \theta \sin^2 \theta + Q_{22} \cos^4 \theta \\
\bar{Q}_{26} &= \left(Q_{11} - Q_{12} - 2Q_{66}\right) \cos \theta \sin^3 \theta - \left(Q_{22} - Q_{12} - 2Q_{66}\right) \cos^3 \theta \sin \theta \\
\bar{Q}_{66} &= \left(Q_{11} + Q_{22} - 2Q_{12} - 2Q_{66}\right) \cos^2 \theta \sin^2 \theta + Q_{66} \left(\cos^4 \theta + \sin^4 \theta\right).
\end{aligned}
\tag{4}
$$

In equation 4, θ is the orientation at which the unidirectional lamina is laid and Q the reduced stiffness matrix:

$$
Q = \begin{bmatrix}
\dfrac{E_{11}^2}{E_{11} - \nu_{12}^2 E_{22}} & \dfrac{\nu_{12} E_{11} E_{22}}{E_{11} - \nu_{12}^2 E_{22}} & 0 \\
\dfrac{\nu_{12} E_{11} E_{22}}{E_{11} - \nu_{12}^2 E_{22}} & \dfrac{E_{11} E_{22}}{E_{11} - \nu_{12}^2 E_{22}} & 0 \\
0 & 0 & G_{12}
\end{bmatrix}
\tag{5}
$$

where E_{11} is the modulus of elasticity across the fibre direction, E_{22} the modulus of elasticity across the transverse direction, G_{12} the shear modulus and ν_{12} the principal Poisson's ratio for a specific material type.

The optimisation algorithm used is NLPQLP [41, 42], a sequential quadratic programming algorithm which is available in the Airbus in-house Multidisciplinary Design and Optimisation platform called *LAGRANGE* [43]. It is worth noting that the optimal stacking sequence attributes are not limited to solely being a function of the structural weight of the structure, but can also take into account performance related metrics such as the Breguet range. Similarly, constraints governing the optimal solution can also include structural eigenmodes or static aeroelastics amongst others. This work focuses on the demonstration of the methodology, therefore the optimisation cases deal with a mass minimisation subject to physical i.e. buckling and strength constraints and composite design and manufacturing constraints. The mathematical formulation of the problem is:

$$
\begin{aligned}
&\text{minimise} \quad \sum_{j=1}^{J}\sum_{i=1}^{I} t_{ij} \\
&\text{subject to} \quad g_k(t) \geq 0 \ \ k \in \{1, \ldots, K\}
\end{aligned}
\tag{6}
$$

where t_{ij} is thickness of the ith layer in patch number j and $g_k(t)$ are the K constraints applied to the optimisation problem.

2.1.2. Physical constraints in gradient-based optimisation

For the examples demonstrated in this work, the plates are assumed to be simply supported, biaxially compressed and specially orthotropic. Buckling constraints in the optimisation are then formulated as:
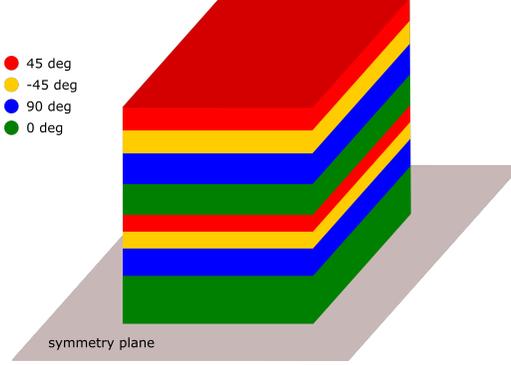
Figure 1: An indicative generic stack of 16 generic plies. Only half of the symmetric stack is shown.

$$\frac{N_x, cr}{N_x} - 1 \geq 0. \tag{7}$$

The fraction in equation 7 will be referred to as a Reserve Factor (RF) and corresponds to the first eigenvalue of the biaxially compressed plate. In equations 7, 8, N_x is the applied load across the longitudinal direction, N_y the load across the transverse direction and $N_{x,cr}$ the critical buckling load in the longitudinal direction which is calculated as:

$$N_{x,cr} = \frac{\pi^2 \left(D_{11} \left(\frac{m}{a} \right)^4 + 2 \left(D_{12} + 2D_{66} \right) \left(\frac{mn}{ab} \right)^2 + 2D_{22} \left(\frac{n}{b} \right)^4 \right)}{\left(\frac{m}{a} \right)^2 + \frac{N_y}{N_x} \left(\frac{n}{b} \right)^2} \tag{8}$$

where a and b are the lengths of the bi-axially loaded plate in the longitudinal and transverse direction respectively. The critical buckling load is the minimum one calculated for a set of m and n half wavelengths across the length and width of the plate respectively. The analytical formula of equation 8 is chosen in this work to maintain consistency when comparing with relevant studies in section 3.3. Since the formula is based on Classical Lamination

Theory the critical buckling load is less accurate for moderately thick and thick laminates.

Concerning strength constraints, the maximum strain criterion is applied in this work for fibre failure. These constraints are formulated as:

$$\left|\frac{\varepsilon_{1T}^u}{\varepsilon_1}\right| - 1 \geq 0 \qquad or \qquad \left|\frac{\varepsilon_{1C}^u}{\varepsilon_1}\right| - 1 \geq 0 \tag{9}$$

for extensional and compressive loads respectively where ε_{1T}^u is the ultimate strain of the material for tension, ε_{1C}^u the ultimate strain for compression and ε_1 is the strain along the fibre direction for a specific generic ply. Knowing the stiffness of a laminate and the force and moment resultants the strain $\boldsymbol{\varepsilon}$ and curvature $\boldsymbol{\kappa}$ distributions can be calculated solving:

$$\begin{Bmatrix} \boldsymbol{N} \\ \boldsymbol{M} \end{Bmatrix} = \begin{bmatrix} \boldsymbol{A} & \boldsymbol{B} \\ \boldsymbol{B} & \boldsymbol{D} \end{bmatrix} \begin{Bmatrix} \boldsymbol{\varepsilon} \\ \boldsymbol{\kappa} \end{Bmatrix}. \tag{10}$$

Once the global strain distribution has been calculated, the strain per ply ε_1 can be computed by transforming the global strain into the local material directions which are known due to using the generic stack to describe the stiffness of the laminate. The reader is invited to further reading on the detailed calculation of strain [44].

2.1.3. Composite constraints in gradient-based optimisation

Aerospace composite components are usually designed to fulfil several composite guidelines that ensure the integrity of the structure by minimising unnecessary coupling behaviours or stress concentrations [45]. It should be noted that such guidelines can be substituted by more generalised classes of laminates [46, 47, 48] or even be ignored when utilising manufacturing

concepts such as Variable Angle Tow laminates [49, 50, 51]. However, these guidelines, which are commonly referred to as composite rules, are still in active use, especially in the aerospace industry, and are grouped in two categories i.e. design and manufacturing rules. Design rules regulate the stacking sequence of a single laminate of constant stiffness. The rules which have been formulated within the scope of this work are briefly described:

1. *Symmetry.* Symmetric laminates about the mid-plane are commonly used to avoid bending-extension coupling. Symmetry can be achieved by linking the design variables on the two sides of the laminate formed by the mid-plane surface.

2. *Balance.* Balanced laminates consist of equal $+\theta$ and $-\theta$ orientations ($\theta \neq 0^o, 90^o$), in order to eliminate shear-extension coupling. Similarly to symmetry, balance may be achieved by linking the design variables corresponding to the $\pm\theta$ oriented layers.

3. *Damage tolerance.* External plies should not be in the direction of the main load. Commonly, a 45° or -45° layer is placed in the outermost part of the laminate. This design rule can be facilitated in the optimisation by choosing a generic stack with a 45° or -45° generic layer on the outer part of the laminate in combination with increasing the minimum gauge of the relevant design variable to the thickness of the tape to be used during manufacturing.

4. *Minimum percentage.* A minimum percentage (p) of any fibre orientation θ_c used in a laminate might be enforced to minimise matrix

degradation and favour a fibre-dominated failure mode instead. This
is mathematically formulated as:

$$p \sum_{i=1}^{I} t_{ij} - \sum_{i'=1}^{I'} t_{i'j} \geq 0 \quad \forall j, i' \in \{I \cap \theta_{ij} = \theta_c\} \tag{11}$$

For laminates in which not only the four standard orientations $(45, -45, 90, 0)$
are used in the design, it does not make sense to apply the minimum
percentage constraint for all fibre orientations [52], as this could lead
to an infeasible design space, but only to the standard ones.

5. *Contiguity.* The maximum grouping of equally oriented layers is lim-
   ited to minimise interlaminar stresses and ensure a homogeneous stress
   distribution. The contiguity design rule applied for a specific θ_c fibre
   orientation is formulated as:

$$\sum_{i'=1}^{I'} \left(\frac{t_{i'j}}{t_d} \right)^n \geq \frac{1}{2} + \frac{1}{2} \tanh\left(k \left(\frac{t_{i^\star j} + t_{(i^\star+1)j}}{t_d} \right) - M - c \right)$$
$$\forall j, i^\star \in \{I \cap \theta_{ij} = \theta_c\}, i^\star < i' < i^\star + 1 \tag{12}$$

The right hand-side of equation 12 is a Heaviside function which takes
values in $[0, 1]$. The design variable driven part of the right hand-side of
the equation captures the total thickness of two 'consecutive' θ_c oriented
plies $i^\star$ and $i^\star + 1$ as shown in Fig. 2. It should be noted that when
referring to the thickness of the generic plies, 'consecutive' does not
imply physical contact but rather the absence of any other θ_c oriented
ply between the two of interest. Anyhow, modelling the laminate using
two generic plies of the same fibre orientation which are in physical

12

contact does not add any advantage but only increases the complexity of the optimisation. When the total thickness of these two 'consecutive' θ_c oriented generic layers becomes larger than the maximum number of allowable consecutive layers of the same fibre orientation M, then the right hand side of the equation increases. Constant t_d denotes the thickness of the tape which will be used in manufacturing, k regulates the steepness of the Heaviside function and c is a tolerance value related with k which defines at which point exactly the sum of the two θ_c oriented plies starts creating a value for the right hand-side of the equation which is 'significantly' larger than zero. The left hand-side of the equation captures the total thickness of all plies placed between the two 'consecutive' θ_c oriented plies. When the right hand-side becomes larger than 0, then the left hand side must also increase to fulfil the constraint meaning that the thicknesses of the intermediate plies must also increase. Exponent n values larger than 1 can be used to enforce a single ply of a specific fibre orientation to be used instead of a collection of plies of various orientations whose thicknesses are smaller than one.

Manufacturing rules, affect the transitioning between laminates placed in neighbouring patches.

1. *Continuity/blending.* Continuity, also commonly referred to as blending ensures manufacturability and structural integrity of the laminated composite. In this work, the definition of generalised blending [53] is used. Generalised blending requires all plies in a thinner patch to continue in the adjacent thicker panels. The mathematical formulation for two neighbouring patches j_1 and j_2 is expressed as:

13

Figure 2: Layer indexing relevant to the contiguity constraint for an indicative subset of generic layers.

$$
\text{if } \sum_{i=1}^{I} t_{ij_1} \leq \sum_{i=1}^{I} t_{ij_2}
$$

$$
\text{then } t_{ij_1} \leq t_{ij_2} \quad \forall i \in I
$$

$$
\text{else } \sum_{i=1}^{I} t_{ij_1} > \sum_{i=1}^{I} t_{ij_2} \tag{13}
$$

$$
\text{then } t_{ij_1} > t_{ij_2} \quad \forall i \in I
$$

2. *Maximum dropping.* The maximum number of plies dropped in transitions between neighbouring laminates j_1 and j_2 is limited, to assist smooth load distribution throughout the structure. On a lamina level this is formulated as:

$$
t_l - |t_{ij_1} - t_{ij_2}| \geq 0 \quad \forall i \in I \tag{14}
$$

and on a laminate level

$$
t_s - \left| \sum_{i=1}^{I} t_{ij_1} - \sum_{i=1}^{I} t_{ij_2} \right| \geq 0. \tag{15}
$$

14

In equations 14 and 15 t_l and t_s are the absolute allowable differences in thickness for a ply and stack respectively.

3. *External covering ply.* At least one of the outer plies in a laminate is not allowed to be dropped to ensure structural integrity. This manufacturing rule can be enforced by setting the minimum gauge of the corresponding design variable to the thickness of the pre-impregnated unidirectional tape.

2.2. Second stage: Discrete optimisation

The optimum continuous solution retrieved by the first stage of the optimisation needs to be converted into a discrete stacking sequence which complies with all the composite design and manufacturing rules. First of all, knowing the thickness of the pre-impregnated tape that will be used for manufacturing, the entire thickness of each generic stack must be rounded-up to either the nearest integer number of plies or the nearest even number of plies. The discrete results presented in this work have been produced after rounding up the total thickness of each patch to the nearest even number of plies. The number of layers for each patch remains constant during the discrete optimisation and the objective for this problem, is minimising the absolute difference between the optimal stiffness provided by the gradient-based optimisation $(\xi_{kj}^{A,B,D})_{\text{optimal}}$ and the stiffness of the computed discrete stack $\xi_{kj}^{A,B,D} \in [-1, 1]$.

$$\min \sum_{j=1}^{J} w_k^{A,B,D} |\xi_{kj}^{A,B,D} - (\xi_{kj}^{A,B,D})_{\text{optimal}}| \quad \forall k \qquad (16)$$

15

It should be noted that once the gradient-based optimisation has converged to the optimal thicknesses of the generic layers, these are converted into lamination parameters allowing a more compact representation of the stiffness attributes of the laminate and easier comparison with similar algorithms available in the literature. In equation 16, weight coefficients $w_k^{A,B,D}$ may be used to emphasise specific stiffness components.

Two different Mixed Integer Linear Programming formulations of the blended stacking sequence optimisation problem, namely explicit and implicit, have been developed by the authors in previous work [40]. The two formulations mainly differ in the way blending is modelled although both provide the same results for a given optimisation problem. For the results presented in this work, the implicit formulation has been employed. To model the stacking sequence optimisation of the structure, both discrete and continuous design variables are used, while the objective function and constraints of the problem are formulated as linear functions with respect to the design variables. The commercial mathematical programming tool Gurobi [54] is used to solve this second stage optimisation problem. A wide range of design and manufacturing rules can be activated depending on the requirements of the design.

3. Results

First of all, the influence of the generic stack initialisation and parametrisation on the retrieved stiffness is demonstrated. Then, discrete results are shown to highlight the accuracy of the applied manufacturing constraints and the importance of having the blending constraint in particular in the con-

16

tinuous optimisation. Finally, the two-stage methodology developed in this work is applied on an academic benchmark problem and compared against previously proposed approaches.

3.1. Constraint demonstration

As mentioned before, parameterising the properties of the laminate using generic stacks introduces local minima in the design space. What is more, the choice of number, stacking sequence and initial thickness of the generic plies can also influence the resulting thickness and stiffness of the structure.

A simple problem consisting of only one panel is examined first. The panel is simply supported along its edges. A graphite-epoxy material (IM7/8552) is used. The modulus of elasticity across the fibre direction is $E_1 = 141GPa$, the modulus of elasticity in the transverse direction is $E_2 = 9.03GPa$, the shear modulus is $G_{12} = 4.27GPa$, the principal Poisson's ratio is $\nu_{12} = 0.32$ and the density is $\rho = 1.572 \times 10^{-6} Kg/mm^3$. The dimensions of the panel and the compressive loads applied are noted in Fig. 3a. Buckling and strength constraints are taken into consideration, initially examining only the first load case of Fig. 3a. The maximum strain criterion of equation 9 is used as a strength constraint. Instead of using the ultimate strain value for the material, a conservative value of the maximum allowable strain ($\varepsilon_{1T}^u = 5500\mu\varepsilon$ and $\varepsilon_{1C}^u = 3000\mu\varepsilon$) taking damage tolerance into consideration is used.

The stacking sequence of the generic stack is $[(45, -45, 90, 0)_4]_s$, combining to a total of 32 generic layers. Symmetry and balance composite constraints are enforced with design variable linking, leading to a total of 12 design variables. Three different schemes, as shown in Table 1, are used to examine the influence of the design variable initialisation on the result.

17
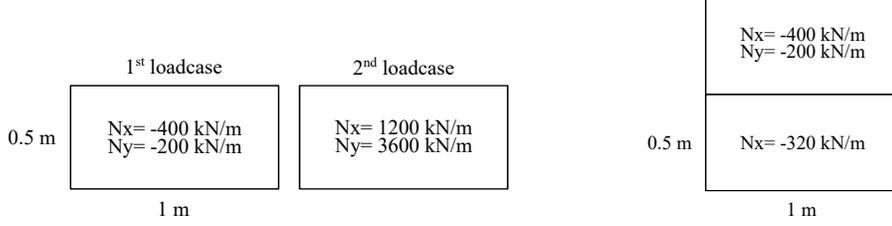
(a) Simply supported panel subject to a compressive and an extensional loadcase respectively.

(b) Simply supported, mechanically disconnected panels subject to compressive loads.

Table 1: Three different initialisation schemes applied to each fibre orientation in the generic plies.

	Initial thickness(mm)			Final mass(Kg)	
Scheme	0°	90°	$\pm45^o$	One load case	Two load cases
1	0.3	0.3	0.3	7.263	7.314
2	0.3	0.3	0.15	7.263	7.314
3	0.15	0.15	0.3	7.262	7.314

In order to visualise the results, the polar representation of the stiffness used by Dillinger et al. [55] and Bordogna et al. [56] is used. The thickness normalised elastic modulus of elasticity rotated 360 degrees around the reference axis of the laminate is calculated as:

$$\hat{E}_{11}\left(\theta\right) = \frac{1}{\hat{A}_{11}^{-1}\left(\theta\right)} \tag{17}$$

The thickness normalised inverse $\hat{A}^{-1}$ matrix as a function of any angle θ is given by:

$$\hat{\mathbf{A}}^{-1}\left(\theta\right) = \mathbf{T}^T\hat{\mathbf{A}}\mathbf{T} \tag{18}$$

where

18

$$\hat{\mathbf{A}} = \frac{\mathbf{A}}{h} \tag{19}$$

and the transformation matrix $\mathbf{T}$

$$\mathbf{T} = \begin{bmatrix} \cos^2\theta & \sin^2\theta & 2\cos\theta\sin\theta \\ \sin^2\theta & \cos^2\theta & -2\cos\theta\sin\theta \\ -\cos\theta\sin\theta & \cos\theta\sin\theta & \cos^2\theta - \sin^2\theta \end{bmatrix}. \tag{20}$$

In equation 17, $\hat{A}_{11}^{-1}(\theta)$ is used to visualise the in-plane stiffness. Similarly, the out-of-plane stiffness can be visualised by using $\hat{D}_{11}^{-1}(\theta)$ with the thickness normalised bending stiffness matrix calculated as:

$$\hat{\mathbf{D}} = \frac{12\mathbf{D}}{h^3}. \tag{21}$$

The resulting in-plane stiffness shown in Fig. 4a is significantly different for each initialisation scheme. On the contrary, out-of-plane stiffnesses (Fig. 4b) are identical for all three schemes. Although the maximum mass difference is at the order of 0.01% (Table 1), the gradient-based optimisation has been trapped in different local minima. The different in-plane stiffnesses indicate different ply-shares between the four fibre orientations. However, since the design is only driven by buckling, the optimiser has computed identical out-of-plane stiffnesses by influencing the distribution of the ply-shares across the thickness of the laminate.

Although local minima due to different initial thicknesses do arise due to the non-convex design space of generic stacks, this drawback is mitigated for real-world problems. When designing aircraft structures, hundreds or thousands of load cases are taken into consideration, depending on the maturity

19

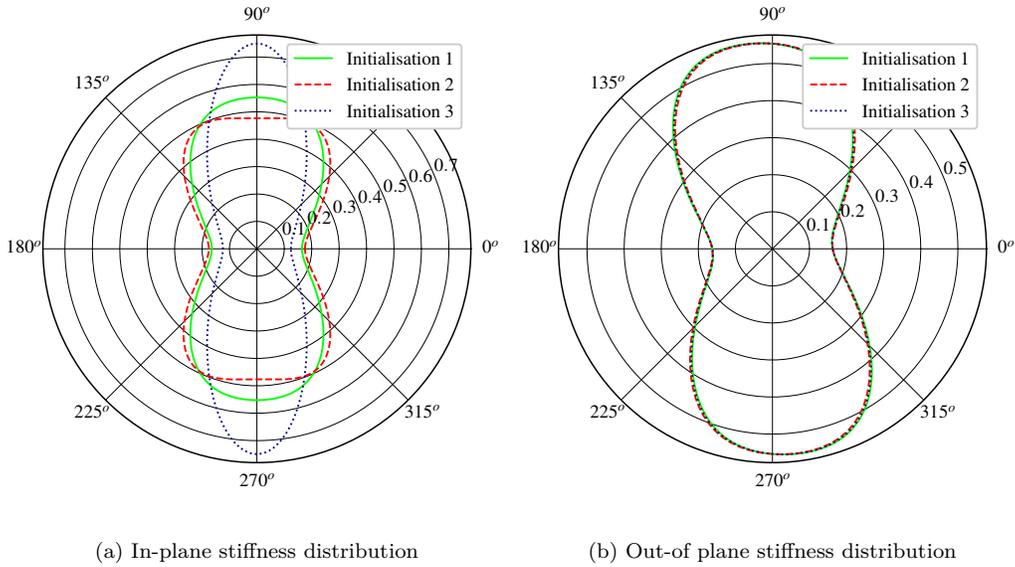(a) In-plane stiffness distribution   (b) Out-of plane stiffness distribution

Figure 4: Comparison of the stiffness distributions for a panel consisting of 32 generic plies subject to buckling loads for different thickness initialisation schemes.

of the design stage, leading to a huge criteria model. The criteria model, consisting of millions of constraints emerging from the design-driving requirements such as strength, damage tolerance, buckling, manufacturing, but also eigenmodes, flutter and aeroelastic effectiveness, is heavily restricting the design space and eliminates, from a practical point of view, the majority of the possible local minima.

To highlight this effect, a second load case of extensive forces along the edges of the panel is also included in the study (Fig. 3b). Examination of the stiffness distributions for the same three initialisation schemes shows identical in-plane stiffness and slightly different out-of-plane stiffness for the first scheme as shown in Figs. 5a and 5b respectively. The masses are equal for all three schemes.

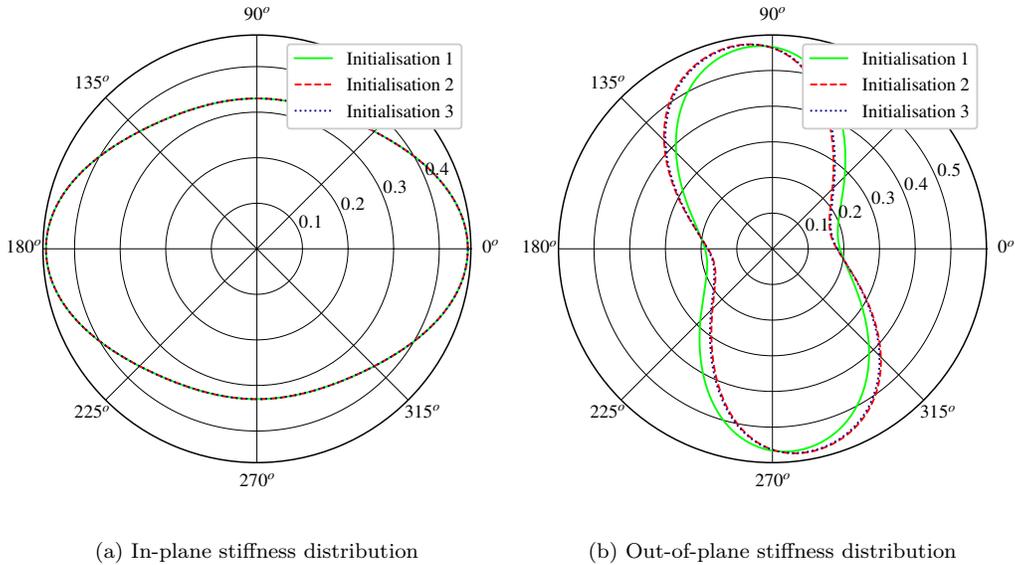(a) In-plane stiffness distribution   (b) Out-of-plane stiffness distribution

Figure 5: Comparison of the stiffness distribution for a panel consisting of 32 generic plies subject to buckling and extensional loads for different thickness initialisation schemes.

The number of generic plies used also influences the computed design. This is demonstrated by optimising the same demo-problem subject to the two load cases and using a different number of the same repetitive generic blocks ($[(45, -45, 90, 0)]$) which form a laminate of 8, 16 and 32 generic layers respectively. Already when using 16 generic plies, the in-plane stiffness of the plate converges to the optimal solution (Fig. 6a) while the out-of-plane stiffness slightly differs between the case of 16 and 32 generic plied as seen in Fig. 6b. Experience gained from application of the two-stage process in many different instances indicates that a laminate which is expected to be approximately N layers thick, can be adequately modelled by a generic stack comprised of $N/4$ generic layers. This modelling guideline is not effective when applying the contiguity manufacturing constraint, where a larger

21

number of generic plies needs to be introduced.

(a) In-plane stiffness distribution
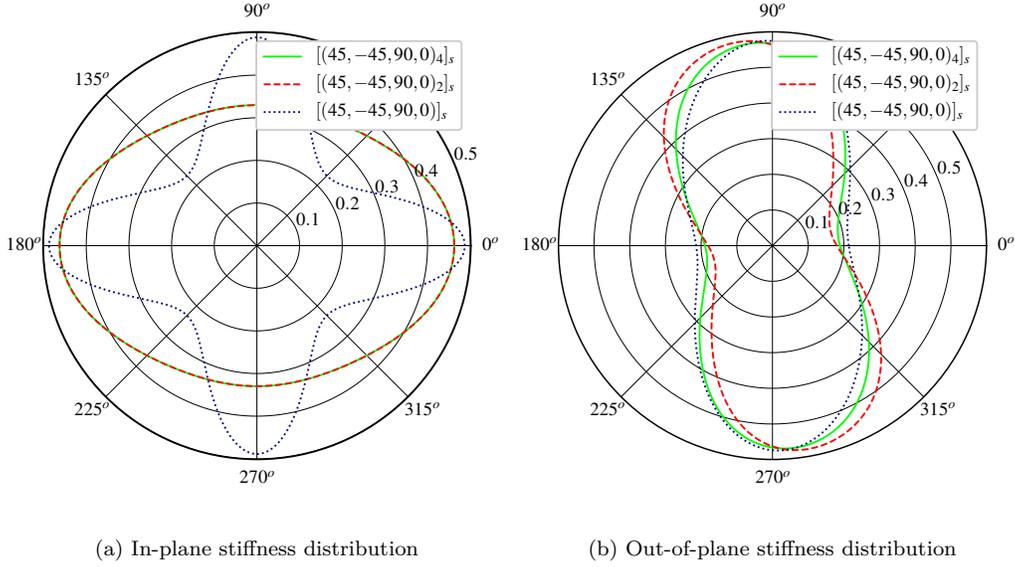
(b) Out-of-plane stiffness distribution

Figure 6: Comparison of the stiffness distributions for a panel consisting of 8, 16 and 32 generic plies subject to buckling and extensional loads.

An additional factor that may influence the resulting membrane and bending stiffness of the laminate is the stacking sequence of the generic block repeated to form the generic stack. In Figs. 7a and 7b the in-plane and out-of-plane stiffness distributions are plotted for the panel when using the $[(0, 90, 45, -45)]$ generic block instead of the one applied for the previous example ($[(45, -45, 90, 0)]$). For each of the blocks, 2 generic stacks are formed, one consisting of 8 generic plies and the other of 16. The resulting stiffnesses of the laminates formed by 8 generic plies are different, which is to be expected since the stiffnesses are also different for the case of 8 and 16 generic layers (Fig. 6). The influence of the repeated generic block on the stiffness ceases when forming a generic stack with 16 layers which supports

22

the previous stiffness sensitivity results with respect to the number of generic plies.

(a) In-plane stiffness distribution
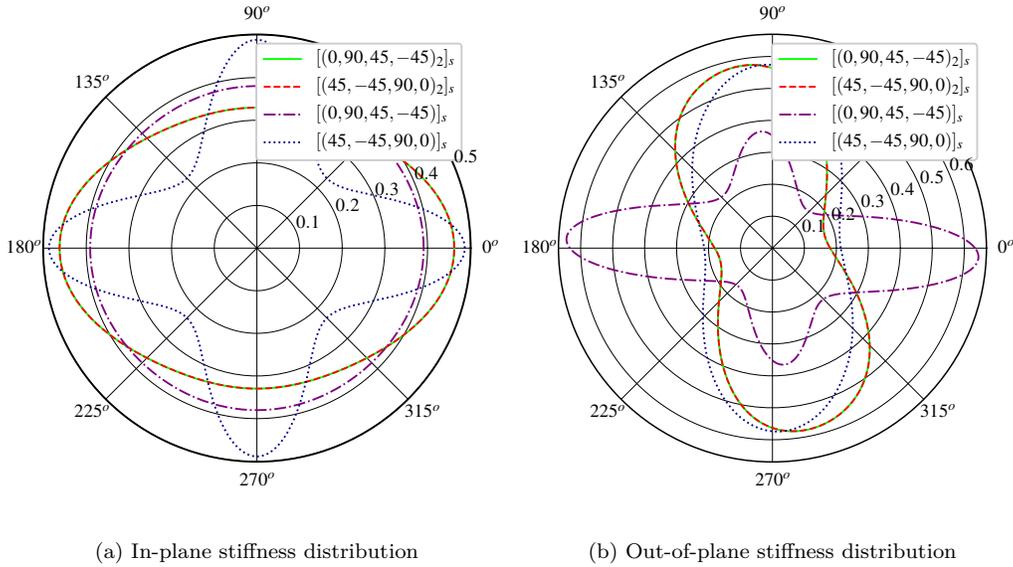
(b) Out-of-plane stiffness distribution

Figure 7: Comparison of the stiffness distributions for a panel comprised of 2 different generic blocks when forming a generic stack of 8 and 16 plies, subject to buckling and extensional loads.

Finally, the influence of the continuity and contiguity constraints on the resulting thickness and stiffness of the structure is reported. A second patch is added to the demonstrator problem to enable the application of the continuity constraint. The two patches are not mechanically connected so no load redistribution is taken into account. Only the continuity constraint couples the design variables of the two patches. A single buckling load case is considered, with the exact loads shown in Fig. 3b.

In Fig. 8a the resulting generic stack of an optimisation not using any composite design or manufacturing rules, besides symmetry and balance, is

23

depicted. The optimum ply-share between the different fibre angles and their distribution across the stack is vastly different. If the contiguity and blending rules are also activated, then this leads to a significantly different structural solution whose stiffness distribution is homogenised (Fig. 8b). As for the application of the contiguity constraint, the assumed discrete ply thickness is 0.125mm and the maximum number of consecutive plies allowed equals 4.
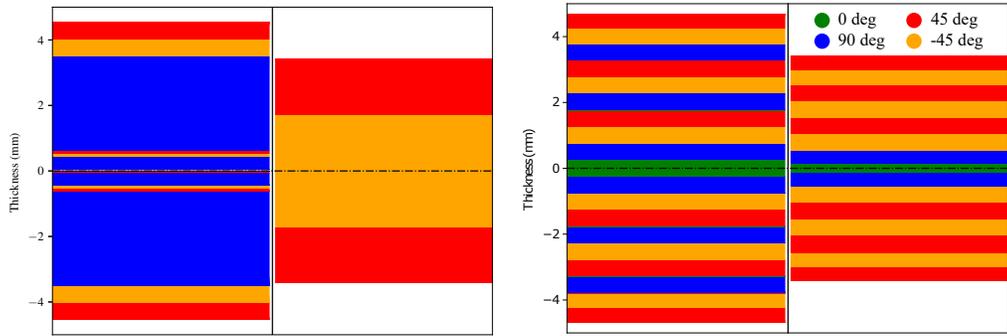
(a) Symmetry and balance design guidelines are enforced

(b) Symmetry, balance, contiguity and blending composite guidelines are enforced

Figure 8: Resultant generic stack thickness distribution for the demonstrator problem of Fig. 3b.

3.2. Importance of continuity constraint

The significance of having the blending constraint in the gradient-based optimisation is demonstrated on the 18-panel horseshoe problem [57] which has been extensively studied in the literature. The panel arrangement, force resultants and dimensions are given in Fig. 9. N_x and N_y force resultants are given in lbf/in ($\times$175.1 to convert into N/m). The same graphite-epoxy

material (IM7/8552) is used whose properties have already been described in section 3.1. The thickness of the ply used is 0.191mm to maintain consistency with other studies.

18 in.		20 in.			
1 $N_x = -700$ $N_y = -400$	2 $N_x = -375$ $N_y = -360$	3 $N_x = -270$ $N_y = -325$	4 $N_x = -250$ $N_y = -200$	5 $N_x = -210$ $N_y = -100$	12 in.

Figure 9: 18 panel horseshoe blending problem [57].

The generic stack used to model the patches in the horseshoe benchmark is $[(45, -45, 90, 0)_3]_s$. The composite constraints applied are symmetry, balance, damage tolerance, a minimum and maximum allowed percentage of 10 and 60 % respectively and the external covering ply rule. If the blending constraint is also applied in the gradient-based optimisation, then the discrete optimisation stage is directly able to retrieve a design which fulfils all buckling constraints. On the contrary, if blending is not enforced in the

25

continuous optimisation stage, the discrete optimiser is not able to retrieve a discrete stacking sequence which satisfies buckling constraints. In such a case, the design factor needs to be increased. This procedure is followed iteratively until the discrete design meets the buckling or any other physical constraints. The outcome of such an iterative effort is demonstrated in Table 2. Consequently, more computational time and manual effort need to be sacrificed. Worst of all, this iterative process leads to a significant weight penalisation, which for this case is 5%. This additional weight is due to overdimensioning several of the patches in the structure as can be seen from the maximum buckling RFs. This goes to show the importance of having as many manufacturing constraints as possible in the gradient-based optimisation stage but also formulating these constraints as accurately as possible.

Table 2: Structural mass and buckling RF comparison for the 18-panel horseshoe problem between a two-stage optimisation in which blending is not included in the first stage and one in which it is activated.

	Continuous results			
	No blending			With Blending
Design factor	1	1.2	1.25	1
Mass(Kg)	27.72	29.45	29.85	28.10
	Discrete results			
Min. Buck. RF	0.83	0.964	1.03	1.01
Max. Buck. RF	1.30	1.60	1.59	1.30
Mass (Kg)	28.93	30.52	30.79	29.31

3.3. Comparison against previous work

In this section, results for the 18-panel horseshoe problem are compared against results achieved by other two-stage optimisation approaches available in the literature. Published results on the benchmark stemming from the application of non-deterministic one-stage approaches [5, 58] are not included because both physical and composite constraints can be included simultaneously. For the current work, the generic stack used is $[(45, -45, 15, -15, 30, -30, 60, -60, 75, -75, 90, 0)_3]_s$, to match the set of fibre angles used by IJsselmuiden et al. [59] and Macquart et al. [20]. In the first stage of the optimisation, besides blending, symmetry is also enforced to ensure no bending-extension coupling exists since this effect is not captured by the analytical buckling formulation of equation 8 used in this work. Likewise, in the discrete optimisation only blending and symmetry are enforced and the allowed fibre orientations are the same as the ones used in the generic stack, which coincide with the ones used in the work of IJsselmuiden et al. [59] and Macquart et al. [20]. Picchi Scardaoni et al. [60] have allowed for any integer fibre orientation to be used in the discrete design. As far as composite design and manufacturing rules are concerned, all three studies [59, 20, 60] have used blending while additionally IJsselmuiden et al. [59] have enforced symmetry and balance and Picchi Scardaoni et al. [60] have applied a manufacturing rule prohibiting small changes in thickness of adjacent panels.

In the work of IJsselmuiden et al. [59], blending constraints were not used in the lamination parameter design space of the gradient-based optimisation. Therefore, the discrete stacking sequence derived initially, significantly violates the buckling RFs. An iterative repair strategy of locally increasing

Table 3: Structural mass and buckling RF comparison for the 18-panel horseshoe problem including blending constraints in the continuous optimisation.

	Mass (Kg)	Min. buckling RF
IJsselmuiden et al. [59]	29.46	1.025
Macquart et al. [20]	28.61	0.979
Picchi Scardaoni et al. [60]	27.28	1.058
Current work	28.15	1.000

thicknesses needs to be performed for several loops until arriving to the end result of Table 3.

In the work of Picchi Scardaoni et al. [60], blending constraints are derived for the polar parameter design space. The design derived by the ant colony optimisation employed for the second optimisation stage is lighter than the one achieved in this work. However, finite element buckling is employed to calculate the buckling RFs of the horseshoe problem instead of the analytical formula of equation 8 employed in this and the other two works [59, 20]. Evaluation of the buckling RFs of the discrete stacks published by the researchers [60] using the analytical expression of equation 8, results in a minimum RF of 0.65. Therefore, due to the different buckling modelling, the resultant masses cannot be fairly compared. Finally, buckling compliant discrete stacks are derived by employing a design factor of 1.1 leading to the minimum RF of 1.058 for the discrete stacks.

The work of Macquart et al. [20] is the one which can be most fairly compared to the results of the proposed methodology. Blending constraints are derived for the lamination parameter design space of the first stage gradient-

based optimisation. The achieved mass of the current work is 1.6% smaller than the one achieved in the work of Macquart et al. [20]. The actual difference should actually be larger, since the reserve factor in the other work [20] is less than 1. Finally, another significant advantage of the present work is that these results are achieved after one pass of the two-stage process. In the lamination parameter space there is the need for a second loop using a design factor of 1.05. At least a third loop which was not performed in the study would eventually be required to satisfy the buckling constraints which would increase the structural weight.

The accuracy of the blending formulation in the generic stacks is further highlighted in Fig. 10. The average difference between the continuous stiffness and the discrete stiffness is noticeably smaller for the current two-stage approach. This smaller distance originates from the accuracy of the blending formulation and leads to manufacturable stacking sequences in one pass of the optimisation process which therefore reduces the mass penalty between the continuous and discrete result. The discrete stacking sequences retrieved in this work, as well as the corresponding buckling RFs are provided in Table 4.

It should be noted that the discrete optimisation stage in this work uses mathematical programming [40] while the other study used a genetic algorithm Macquart [61]. Differences not related to the algorithmic side of the two second-stage approaches, but rather to the design freedom of each blending formulation, do exist, with the discrete optimisation of the current work having more flexibility. A quantification of the percentage each of the continuous and discrete optimisation contribute to a lower structural mass has not
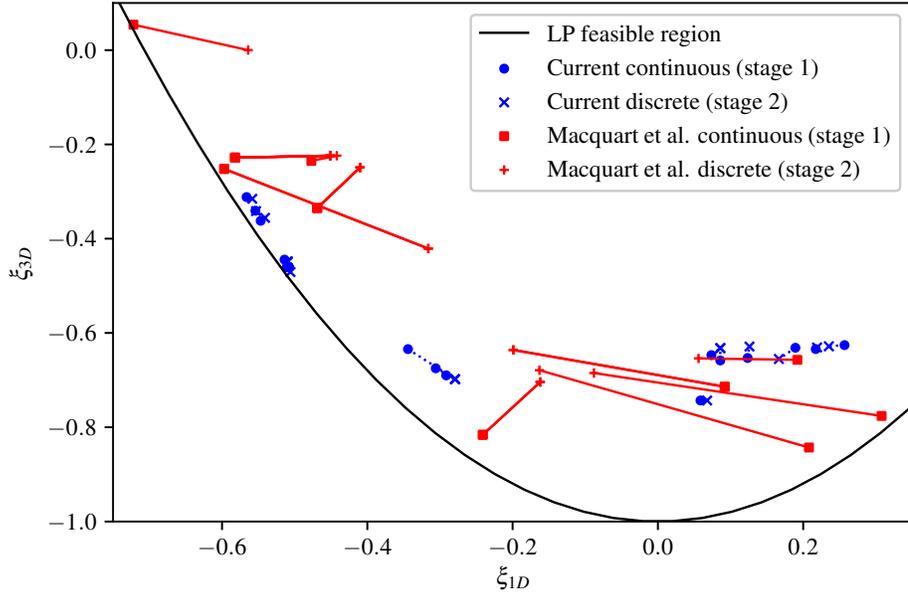
Figure 10: Continuous and discrete results of the current work and of Macquart et al. [20] depicted in lamination parameter (ξ_{1D}, ξ_{3D}) space. For the mathematical formulation of the lamination parameters the reader is invited to further reading [20].

been performed. However, results of section 3.2 confirm that the ability of getting buckling constraint satisfaction in one pass of the optimisation process significantly drives mass down and therefore part of the lower structural mass can be attributed to using generic stacks.

4. Conclusion

This paper introduces a two-stage approach to the optimisation of composite structures taking into account composite design and manufacturing rules. In the first gradient-based optimisation stage, the properties of the

Table 4: Optimal discrete stacks and the corresponding buckling RFs.

Patch	No. of layers	Stacking sequence	Buckling RF
1	34	[-30,30,45,30,-45,30,-45,60,60,45,-60,60,-60,-75,-45,90,45]$_s$	1.160
2	28	[-30,45,30,-45,30,60,60,-60,60,-60,-75,-45,90,45]$_s$	1.012
3	22	[45,-45,60,60,-60,60,-60,-75,-45,90,45]$_s$	1.222
4	18	[60,60,-60,60,-60,-75,-45,90,45]$_s$	1.040
5	16	[60,60,-60,60,-60,-75,-45,45]$_s$	1.207
6	22	[45,-45,60,60,-60,60,-60,-75,-45,90,45]$_s$	1.099
7	18	[60,60,-60,60,-60,-75,-45,90,45]$_s$	1.007
8	24	[60,60,-60,60,-60,-75,75,-60,90,-45,90,45]$_s$	1.032
9	38	[-30,30,30,45,30,-45,30,-45,60,-30,60,45,-60,60,-60,-75,-45,90,45]$_s$	1.056
10	36	[-30,30,30,45,30,-45,30,-45,60,60,45,-60,60,-60,-75,-45,90,45]$_s$	1.143
11	30	[-30,45,30,-45,30,60,-30,60,-60,60,-60,-75,-45,90,45]$_s$	1.083
12	28	[-30,45,30,-45,30,60,60,-60,60,-60,-75,-45,90,45]$_s$	1.007
13	22	[45,-45,60,60,-60,60,-60,-75,-45,90,45]$_s$	1.150
14	18	[60,60,-60,60,-60,-75,-45,90,45]$_s$	1.103
15	24	[60,60,-60,60,-60,-75,75,90,-45,90,-60,45]$_s$	1.000
16	32	[45,-30,-45,45,30,-45,30,60,60,-60,60,-60,-75,-45,90,45]$_s$	1.056
17	18	[60,60,-60,60,-60,-75,-45,90,45]$_s$	1.021
18	22	[60,60,-60,60,-60,-75,90,-45,90,-60,45]$_s$	1.065

structure are modelled using generic stacks, with an emphasis on the implementation of discrete composite design and manufacturing guidelines in this continuous design space. The second stage of the optimisation involves mathematical programming which solves a Mixed Integer Linear Programming formulation of the stacking sequence optimisation subject to any composite rule, aiming to accurately match the continuous optimisation stiffness characteristics.

More specifically, this work focuses on the formulation of as many composite guidelines in the continuous optimisation as possible. The design space of generic stacks allows for more composite rules to be implemented, since it is a direct representation of the stack's sequence characteristics. Moreover, these formulations are more precise compared to the other modelling approaches, such as, lamination and polar parameters. Blending, in particular, can be exactly described in its continuous form. However, generic stacks do form a non-convex design space which is not welcome in any gradient-based optimisation. The influence of different starting points in the retrieved result is expected to be eliminated by the diversity of factors sizing real-world composite structures. The effect of the number of generic plies on the final stiffness distribution is also investigated, indicating that even for industrial scale structures which are expected to be thicker, the size of the continuous optimisation will still remain manageable.

Finally, the importance of having an accurate blending formulation in the continuous optimisation is demonstrated by comparing the results from both including and excluding the constraint from the gradient-based optimisation. In the case that the constraint is included, the computational effort is reduced

to the minimum as there is not need to perform extra two-stage optimisation loops and additionally significant weight savings are achieved. The presented two-stage approach is also applied on a widely used benchmark and is compared against other similar studies using lamination and polar parameters. The current methodology leads to a lower structural weight compared to previous works having used the same hypothesis for the benchmark. Moreover, the proposed two-stage methodology results in composite structures satisfying both discrete composite requirements but also buckling constraints after a single pass of the two stages

5. Acknowledgements

6. Author statement

G. Ntourmas: Conceptualization, Methodology, Software, Formal analysis, Writing-Original Draft, Writing-Review & Editing. **F. Glock**: Conceptualization, Software, Supervision, Writing-Review & Editing. **F. Daoud**: Conceptualization, Supervision. **G. Schuhmacher**: Conceptualization, Supervision. **D. Chronopoulos**: Supervision, Writing-Review & Editing, Funding acquisition. **E. Özcan**: Supervision, Writing-Review & Editing

7. Declaration of Interests

The authors declare that they have no known competing financial interests or personal relationships that could have appeared to influence the work reported in this paper.

8. Data availability

The data that support the findings of this study are available on request from the corresponding author.

References

[1] H. Ghiasi, D. Pasini, L. Lessard, Optimum stacking sequence design of composite materials part i: Constant stiffness design, Composite Structures 90 (2009) 1–11.

[2] H. Ghiasi, K. Fayazbakhsh, D. Pasini, L. Lessard, Optimum stacking sequence design of composite materials part ii: Variable stiffness design, Composite Structures 93 (2010) 1–13.

[3] R. Le Riche, R. Haftka, Optimization of laminate stacking sequence for buckling load maximization by genetic algorithm, AIAA Journal 31 (1993) 951–956.

[4] A. Todoroki, R. Haftka, Stacking sequence optimization by a genetic algorithm with a new recessive gene like repair strategy, Composites Part B: Engineering 29 (1998) 277–285.

[5] F.-X. Irisarri, A. Lasseigne, F.-H. Leroy, R. Le Riche, Optimal design of laminated composite structures with ply drops using stacking sequence tables, Composite Structures 107 (2014) 559–569.

[6] M. Montemurro, Y. Koutsawa, S. Belouettar, A. Vincenti, P. Vannucci, Design of damping properties of hybrid laminates through a global optimisation strategy, Composite Structures 94 (2012) 3309–3320.

[7] M. I. Izzi, M. Montemurro, A. Catapano, J. Pailhès, A multi-scale two-level optimisation strategy integrating a global/local modelling approach for composite structures, Composite Structures 237 (2020) 111908.

[8] F. Aymerich, M. Serra, Optimization of laminate stacking sequence for maximum buckling load using the ant colony optimization (aco) meta-heuristic, Composites Part A: Applied Science and Manufacturing 39 (2008) 262–272.

[9] N. Chang, W. Wang, W. Yang, J. Wang, Ply stacking sequence optimization of composite laminate by permutation discrete particle swarm optimization, Structural and Multidisciplinary Optimization 41 (2010) 179–187.

[10] O. Erdal, F. O. Sonmez, Optimum design of composite laminates for maximum buckling load capacity using simulated annealing, Composite Structures 71 (2005) 45 – 52.

[11] F. Javidrad, M. Nazari, H. Javidrad, Optimum stacking sequence design of laminates using a hybrid pso-sa method, Composite Structures 185 (2018) 607–618.

[12] S. Grihon, Structure sizing optimization capabilities at airbus, in: A. Schumacher, T. Vietor, S. Fiebig, K.-U. Bletzinger, K. Maute (Eds.), Advances in Structural and Multidisciplinary Optimization, Springer International Publishing, Cham, 2018, pp. 719–737.

[13] S. Zein, P. Basso, S. Grihon, A constraint satisfaction programming approach for computing manufacturable stacking sequences, Computers and Structures 136 (2014) 56–63.

[14] S. Zein, V. Madhavan, D. Dumas, L. Ravier, I. Yague, From stacking sequences to ply layouts: An algorithm to design manufacturable composite structures, Composite Structures 141 (2016) 32–38.

[15] S. W. Tsai, N. J. Pagano, Invariant properties of composite materials, in: Composite Materials Workshop, 1968.

[16] S. IJsselmuiden, Optimal Design of Variable Stiffness Composite Structures using Lamination Parameters, Ph.D. thesis, TU Delft, 2011.

[17] S. Setoodeh, M. Abdalla, Z. Gürdal, Approximate feasible regions for lamination parameters, volume 2, 2006, pp. 814–822.

[18] X. Liu, C. A. Featherston, D. Kennedy, Two-level layup optimization of composite laminate using lamination parameters, Composite Structures 211 (2019) 337 – 350.

[19] C. Diaconu, M. Sato, H. Sekine, Feasible region in general design space of lamination parameters for laminated composites, AIAA Journal 40 (2002) 559–565.

[20] T. Macquart, M. Bordogna, P. Lancelot, R. De Breuker, Derivation and application of blending constraints in lamination parameter space for composite optimisation, Composite Structures 135 (2016) 224–235.

[21] T. Macquart, V. Maes, M. Bordogna, A. Pirrera, P. Weaver, Optimisation of composite structures – enforcing the feasibility of lamination parameter constraints with computationally-efficient maps, Composite Structures 192 (2018) 605–615.

[22] S. Ijsselmuiden, M. Abdalla, Z. Gürdal, Implementation of strength-based failure criteria in the lamination parameter design space, AIAA Journal 46 (2008) 1826–1834.

[23] F.-X. Irisarri, C. Julien, D. Bettebghor, F. Lavelle, Y. Guerin, K. Mathis, A general optimization strategy for composite sandwich structures, Structural and Multidisciplinary Optimization 63 (2021) 3027–3044.

[24] J. L. Grenestedt, P. Gudmundson, Lay-up optimization of composite material structures, in: IUTAM Symposium on Optimal Design with Advanced Materials, 1993.

[25] D. Bettebghor, N. Bartoli, Approximation of the critical buckling factor for composite panels, Structural and Multidisciplinary Optimization 46 (2012) 561–584.

[26] M. Montemurro, A. Pagani, G. Fiordilino, J. Pailhès, E. Carrera, A general multi-scale two-level optimisation strategy for designing composite stiffened panels, Composite Structures 201 (2018) 968–979.

[27] M. Montemurro, A. Vincenti, P. Vannucci, A two-level procedure for the global optimum design of composite modular structures—application to the design of an aircraft wing part i, Journal of Optimization Theory and Applications 155 (2012) 1–23.

[28] E. Panettieri, M. Montemurro, A. Catapano, Blending constraints for composite laminates in polar parameters space, Composites Part B: Engineering 168 (2019) 448 – 457.

[29] A. Catapano, B. Desmorat, P. Vannucci, Stiffness and strength optimization of the anisotropy distribution for laminated structures, Journal of Optimization Theory and Applications 167 (2015) 118–146.

[30] M. Picchi Scardaoni, M. Montemurro, Convex or non-convex? on the nature of the feasible domain of laminates, European Journal of Mechanics - A/Solids 85 (2021).

[31] H. Mateus, C. Soares, C. Soares, Buckling sensitivity analysis and optimal design of thin laminated structures, Computers & Structures 64 (1997) 461 – 472.

[32] L. A. Schmit Jnr., B. Farshi, Optimum laminate design for strength and stiffness, International Journal for Numerical Methods in Engineering 7 (1973) 519–536.

[33] D. Costin, B. Wang, Optimum design of a composite structure with manufacturing constraints, Thin-Walled Structures 17 (1993) 185 – 202.

[34] J. Sjølund, E. Lund, Structural gradient based sizing optimization of

wind turbine blades with fixed outer geometry, Composite Structures 203 (2018) 725 – 739.

[35] J. Stegmann, E. Lund, Discrete material optimization of general composite shell structures, International Journal for Numerical Methods in Engineering 62 (2005) 2009–2027.

[36] E. Lund, J. Stegmann, On structural optimization of composite shell structures using a discrete constitutive parametrization, Wind Energy 8 (2005) 109–124.

[37] S. N. Sørensen, R. Sørensen, E. Lund, Dmto – a method for discrete material and thickness optimization of laminated composite structures, Structural and Multidisciplinary Optimization 50 (2014) 25–47.

[38] J. H. Sjølund, D. Peeters, E. Lund, A new thickness parameterization for discrete material and thickness optimization, Structural and Multidisciplinary Optimization 58 (2018) 1885–1897.

[39] D. Liu, V. Toropov, O. Querin, D. Barton, Bilevel optimization of blended composite wing panels, Journal of Aircraft 48 (2011) 107–118.

[40] G. Ntourmas, F. Glock, F. Daoud, G. Schuhmacher, D. Chronopoulos, E. Özcan, Mixed integer linear programming formulations of the stacking sequence and blending optimisation of composite structures, Composite Structures 264 (2021) 113660.

[41] K. Schittkowski, Nlpql: A fortran subroutine solving constrained nonlinear programming problems, Annals of Operations Research 5 (1986) 485–500.

[42] K. Schittkowski, A robust implementation of a sequential quadratic programming algorithm with successive error restoration, Optimization Letters 5 (2011) 283–296.

[43] G. Schuhmacher, F. Daoud, O. Petersson, M. Wagner, Multidisciplinary airframe design optimisation, in: 28th International Congress of the Aeronautical Sciences, volume 1, 2012, pp. 44–56.

[44] M. R. Jones, Mechanics of Composite Materials, CRC press, 1999.

[45] J. Bailie, R. Ley, A. Pasricha, A summary and review of composite laminate design guidelines, National Aeronautics and Space Administration, Final (1997).

[46] P. Vannucci, G. Verchery, A special class of uncoupled and quasi-homogeneous laminates, Composites Science and Technology 61 (2001) 1465–1473.

[47] M. Montemurro, An extension of the polar method to the first-order shear deformation theory of laminates, Composite Structures 127 (2015) 328–339.

[48] M. Montemurro, The polar analysis of the third-order shear deformation theory of laminates, Composite Structures 131 (2015) 775–789.

[49] G. Raju, Z. Wu, B. C. Kim, P. M. Weaver, Prebuckling and buckling analysis of variable angle tow plates with general boundary conditions, Composite Structures 94 (2012) 2961–2970.

[50] M. Montemurro, A. Vincenti, P. Vannucci, Design of the elastic properties of laminates with a minimum number of plies, Mechanics of Composite Materials 48 (2012) 369–390.

[51] M. Montemurro, A. Catapano, A general b-spline surfaces theoretical framework for optimisation of variable angle-tow laminates, Composite Structures 209 (2019) 561–578.

[52] M. Abdalla, C. Kassapoglou, Z. Gürdal, Formulation of composite laminate robustness constraint in lamination parameters space, 2009.

[53] J. V. Campen, O. Seresta, M. Abdalla, Z. Gürdal, General blending definitions for stacking sequence design of composite laminate structures, in: 49th AIAA/ASME/ASCE/AHS/ASC Structures, Structural Dynamics, and Materials Conference, 2012.

[54] L. Gurobi Optimization, Gurobi Optimizer Reference Manual, 2018.

[55] J. Dillinger, T. Klimmek, M. Abdalla, Z. Gürdal, Stiffness optimization of composite wings with aeroelastic constraints, Journal of Aircraft 50 (2013) 1159–1168.

[56] M. Bordogna, P. Lancelot, D. Bettebghor, R. De Breuker, Static and dynamic aeroelastic tailoring with composite blending and manoeuvre load alleviation, Structural and Multidisciplinary Optimization 61 (2020) 2193–2216.

[57] G. Soremekun, Z. Gürdal, C. Kassapoglou, D. Toni, Stacking sequence blending of multiple composite laminates using genetic algorithms, Composite Structures 56 (2002) 53–62.

[58] J. Yang, B. Song, X. Zhong, P. Jin, Optimal design of blended composite laminate structures using ply drop sequence, Composite Structures 135 (2016) 30–37.

[59] S. IJsselmuiden, M. Abdalla, O. Seresta, Z. Gürdal, Multi-step blended stacking sequence design of panel assemblies with buckling constraints, Composites Part B: Engineering 40 (2009) 329–336.

[60] M. Picchi Scardaoni, M. Montemurro, E. Panettieri, A. Catapano, New blending constraints and a stack-recovery strategy for the multi-scale design of composite laminates, Structural and Multidisciplinary Optimization (2020).

[61] T. Macquart, Optibless - an open-source toolbox for the optimisation of blended stacking sequences, 2016.